

# Feasibility of Harvesting Power to Run a Domestic Water Meter Using Streaming Cell Technology

Mark H. Jones and Jonathan Scott

**Abstract**—We investigate the possibility of using streaming cells as a means of harvesting energy from the town water supply. We measure the electrical power developed from streaming cells using tap water as a working fluid. We estimate the amount of energy available from a typical domestic household based on water usage data. We estimate the amount of energy required to operate a simple data logger and transmitter. From these estimates we calculate the required efficiency and physical form of a streaming cell energy converter. We comment on the feasibility of using streaming cell technology as a means of harvesting energy from a domestic water supply.

## I. INTRODUCTION

Domestic and commercial water metering is becoming increasingly common throughout the world. [1] Cheap and reliable methods for retrieving metered data are important for water utility companies.

The introduction of wireless automatic meter reading systems offers many advantages to suppliers of town water. These include increased billing frequency, leak detection and removal of the need to access consumers' property. [1], [2]

The location of a typical water meter means electrical power is usually provided by long life batteries. The batteries used in automatic meter readers are non-rechargeable and have a life-span of around 10 years. [3] Removing batteries from meter reading systems will reduce both the total cost of ownership and electrical waste.

Streaming cells provide a way of converting fluid energy into electrical energy without moving parts. They work on the principle that charged surfaces in contact with ionic solutions attract counter-ions so as to form a charged layer at the contact surface. [4] This charged layer is termed the interfacial double layer and is the key mechanism that enables streaming cell energy conversion. The conversion is made by forcing ions within the double layer through narrow channels by applying hydrostatic pressure.

A double layer is comprised of two individual layers; the *compact* and *diffuse* layers. The compact layer refers to immobilised counter-ions bound directly to the liquid-solid interface. [5] The diffuse layer surrounds the compact layer and contains counter-ions that are not so strongly bound as to be immobile. The thickness of the double layer is defined as the Debye length ( $l_D$ ) and is dependant upon the ionic concentration of the liquid and the electric potential on the solid surface. [6] When the dimensions of a streaming cell channel become small enough, double layers will overlap. Overlapping double layers mean that any co-ions are repelled from within the channel. A simplified diagram showing counter-ions being forced through a streaming cell channel is presented as Fig. 1.

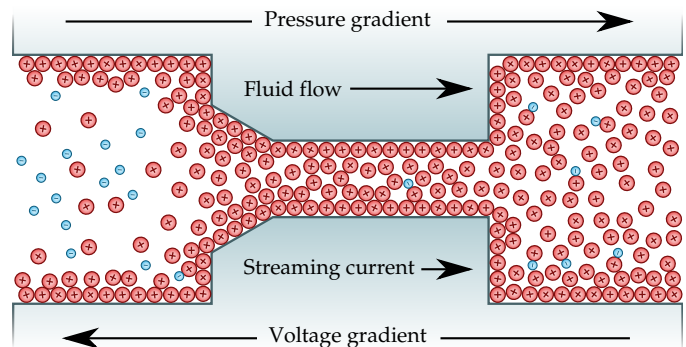


Fig. 1. Conceptualised rendering of the cross section of a streaming cell. Positive ions are being forced through the cavity by the application of pressure.

Channels can be created individually using a range of fabrication methods, such as chemical etching or using narrowly separated parallel plates. They can also be formed en-mass by using porous materials such as glass or ceramics, where the pores themselves act as channels.

Glass has the attractive property that it obtains a negative surface charge when in contact with water. This surface charge is caused by the deprotonation of surface silanol groups in glass ( $\text{SiOH} \rightleftharpoons \text{SiO}^- + \text{H}^+$ ). [7] By immersing a glass channel in an electrolyte solution, double layers of counter-ions (positive ions in this case) occupy the interior walls of the channel.

Counter-ions within a streaming cell are transported by applying a pressure gradient across the channel. Pressure forces the counter-ion rich fluid through the channel creating a current of ions, termed the streaming current. Streaming currents establish a voltage across the cell, termed streaming potential, due to ionic concentrations at each end of the channel becoming unbalanced.

Streaming currents have been heavily investigated as a means of generating electrical energy from pressure gradients. [8]–[23] Theoretical predictions of the efficiency of standard micro/nano-fluidic channels are 2% for pure water and 7% for sodium chloride. [20] Experimental results show conversion efficiencies in the range of:

- 0.01% by forcing water through porous glass with pore sizes from 10–16  $\mu\text{m}$ . [23]
- 0.8% by forcing pure water through a ceramic rod populated with 6  $\mu\text{m}$  pores. [24]
- 3% by forcing a sodium chloride solution through a 75 nm by 50  $\mu\text{m}$  silica channel. [21]
- 0.77% by forcing a sodium chloride solution through a 200 nm pore in an alumina membrane. [15]

- 5% by forcing a sodium chloride solution through a 0.5 nm cylindrical pore in polyethylene terephthalate foil. [22]

These results indicate that small channels using solutions containing salt are more efficient. According to [10], the efficiency is maximised when the channel height twice that of the Debye length. Additionally, [20] states that the maximum efficiency is found when the salt concentration is low.

It is clear from the literature that there is significant progress to be made with respect to increasing the conversion efficiency of streaming cells. Techniques to induce hydrodynamic slip at the fluid-solid interface are predicted to increase this efficiency to 30-40%. [11], [19] Experimental results utilising slip enhanced channels have not yet been reported in the literature. This type of enhancement would overcome the ‘no-slip boundary condition’ at the solid-liquid interface. Slip would mean that ions in the compact layer, where ionic concentration is highest, could also be moved through the channel. Surface enhanced channels are out of the scope of this study due to cost and manufacturing difficulty.

We address the question of whether it is feasible to build a harvester using readily available materials. Such a harvester must produce enough energy to operate a microprocessor and radio communication device. It must collect all of its energy from a domestic water supply without noticeably affecting the supply, and be reliable.

The remainder of this work is presented as follows. In section II we build, measure, and calculate the conversion efficiency of a simple streaming potential cell. We confirm the relationship between voltage and applied pressure and investigate the effect of channel height. In section III we estimate the amount of harvestable energy from a domestic water usage profile. Section IV quantifies energy requirements of a simple electronic meter reader with a wireless transmitter. In section V we calculate the physical size of a harvester intended for electronic meter reading. And finally, we conclude with a discussion on the feasibility of using streaming cells to harvest energy.

## II. READILY ATTAINABLE STREAMING CELL EFFICIENCY

In [25], the authors employ a relatively simple parallel plate design to create a streaming cell. They glued plastic shims between parallel plates of glass, providing a simple way of setting a channel’s height. Using that method, the authors fabricated three cells with internal channel heights of 50  $\mu\text{m}$ , 100  $\mu\text{m}$  and 150  $\mu\text{m}$ . Each of the channels were 3 cm long and had an internal width of 1 cm.

We replicate the approximate dimensions of [25] to produce ten streaming cells. The approximate internal heights of these channels are 245  $\mu\text{m}$ , 178  $\mu\text{m}$ , 161  $\mu\text{m}$ , 125  $\mu\text{m}$ , 106  $\mu\text{m}$ , 75  $\mu\text{m}$ , 71  $\mu\text{m}$ , 56  $\mu\text{m}$ , 52  $\mu\text{m}$ , and 26  $\mu\text{m}$ . The channels are made from glass microscope slides (Sail Brand - JIA 7101WT) sectioned into halves. Plastic shims (Garlock Colorplast) are epoxied (Selleys Araldite Ultra Clear Resin) between slide halves to separate the slides. The dimensions at each end of each channel are measured under a microscope to determine the channel height once the epoxy resin has set.

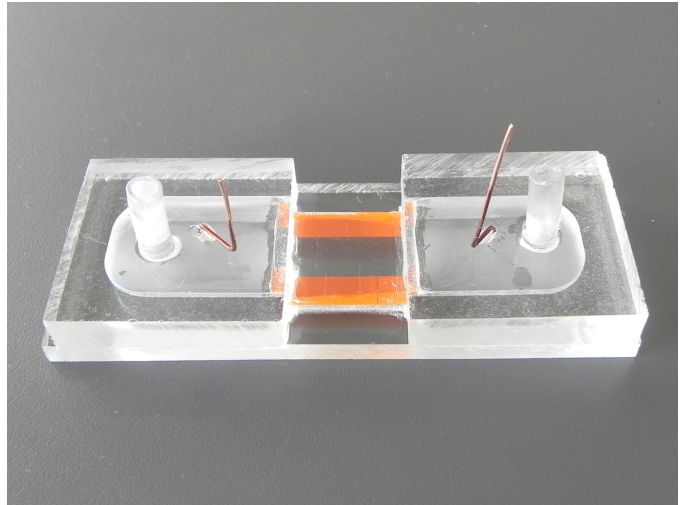


Fig. 2. One of ten constructed streaming cells mounted in an acrylic holder. Copper wires have been epoxied into each side to provide a means of measuring the developed potential across the cell. The plastic shims are visible as the orange strips at each side of the cell.

Each channel is then epoxied between two acrylic reservoirs and a base plate. This gives a rigid structure under pressure and allows the connection of copper wires and rubber hoses. A photo of one of the cells is shown in Fig. 2.

Pressure is applied to the cell by applying mains water pressure to one end while leaving the the other open to atmosphere. A Honeywell pressure sensor (model 26PC15SMT) is placed across the cell to measure applied pressure. An Agilent precision measurement mainframe (model E5270B) is used to measure the streaming potential, streaming current and the pressure sensor’s output. The working fluid, being tap water, had a conductivity of 183  $\mu\text{S cm}^{-1}$  as measured with an EDT Instruments RE 388Tx Conductivity Meter.

Measured pressure-to-voltage gradients from each of the ten streaming cells are presented in Fig. 3. Spread in the data is attributed to uncertainty in the internal dimensions of each cell. Due to the opacity of the resin used, measurement of the internal cell widths was not possible. The plot shows the relationship between channel height and voltage gradient per Pascal of applied pressure. Each cell also had a different flow rate, which this plot does not take into account. Unfortunately, three of the cells burst before flow measurements could be obtained.

We now measure available power output of the 71  $\mu\text{m}$  streaming cell. This cell was chosen as it remained mechanically robust and had good output characteristics. We measure the streaming voltage and pressure while sweeping the electrical current drawn from the device. The applied pressure was held at 260 kPa for the duration of the measurement and the flow rate was previously determined to be 2.05  $\text{ml s}^{-1}$ .

Fig. 5 shows the measured data along with the calculated power. Using the power curve we calculate the cell’s internal electrical resistance to be 5.6  $\text{M}\Omega$ . Peak output power of 1.52 nW is delivered when the current draw is 33.5 nA with a voltage of 182 mV.

By calculating the power provided to the harvester and

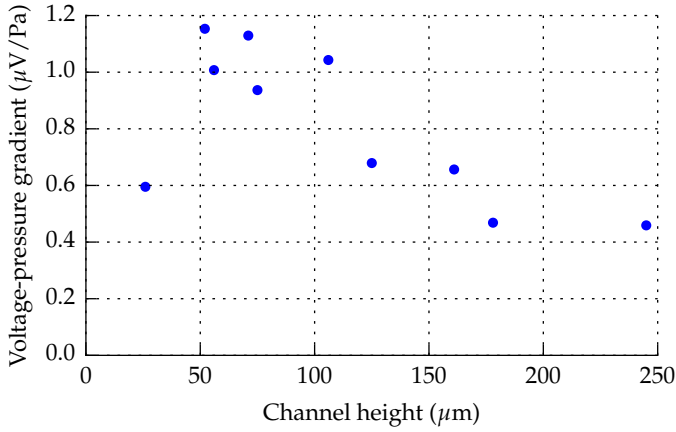


Fig. 3. Gradient of developed streaming voltage with applied pressure differential versus the channel height of ten fabricated streaming cells.

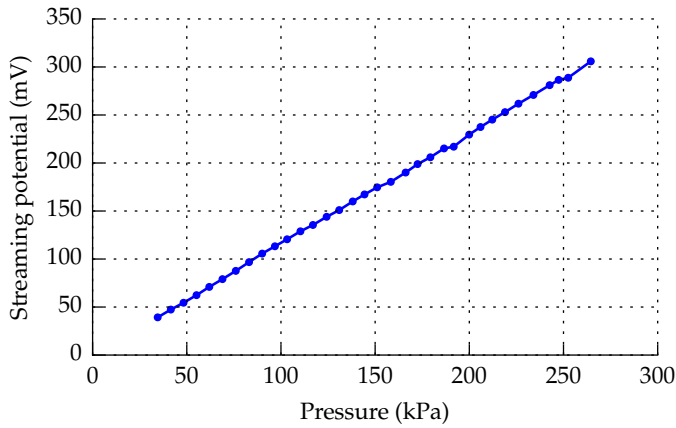


Fig. 4. Measured voltage developed across the 52 $\mu\text{m}$  streaming cell as a function of the differential pressure across the cell.

knowing the power output we calculate the cell efficiency.

$$P_{in} = 260 \text{ kPa} \cdot 2.05 \times 10^{-6} \text{ m}^3 \text{ s}^{-1} = 533 \text{ mW} \quad (1)$$

$$P_{out} = 1.53 \text{ nW} \quad (2)$$

$$\epsilon = \frac{P_{out}}{P_{in}} = 2.87 \times 10^{-9} = 0.287 \mu\% \quad (3)$$

Energy conversion efficiency is in the order of  $0.3 \mu\%$ . While the conversion efficiency is much lower than those stated in the introduction, we use much larger channel dimensions.

### III. ESTIMATION OF HARVESTABLE ENERGY FROM A TYPICAL NEW ZEALAND DWELLING

In [26] the authors monitor water consumption of 51 homes throughout Auckland, New Zealand between February and September of 2008. The report shows that the majority of domestic water is consumed by the shower (30%), washing machine (27%) and toilet (20%). Together these account for over three quarters of the indoor water usage in the average home.

We have created a flow profile, using data from both [26] and [27], from which to calculate the available energy. The

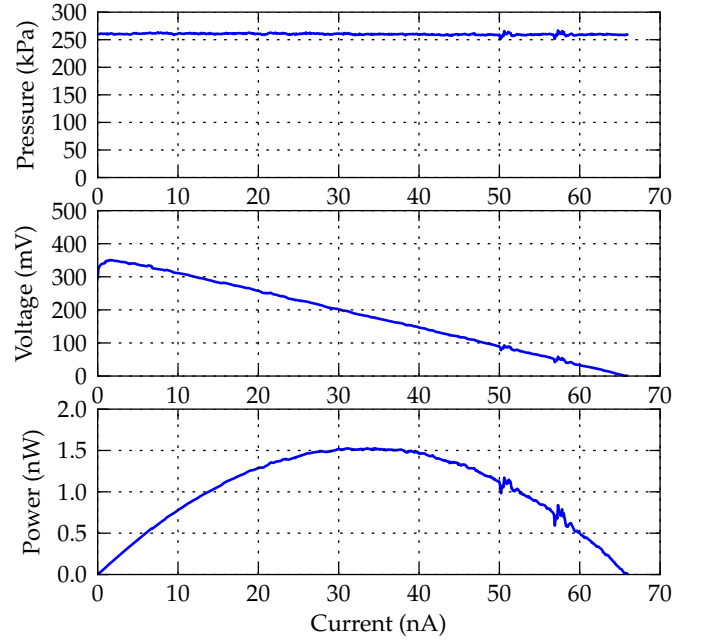


Fig. 5. Streaming cell output voltage as a function of drawn current with constant pressure. The cell's calculated output power appears in the lower plot with a peak at approximately 33.5 nA.

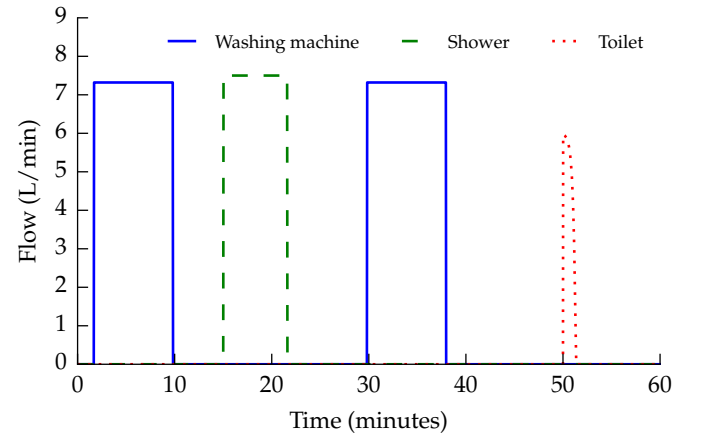


Fig. 6. Sample profile showing constructed instances of washing machine use, a shower and a toilet flush. Washing machine usage is broken into two parts corresponding to a wash and rinse cycle.

profile fits the usage statistics of a home with two occupants according to the previously mentioned reports over the duration of a week. During that time five uses of a washing machine, fourteen showers and fifty six toilet flushes occur. A sample of the usage profiles of each item is shown in Fig. 6.

Fig. 7 shows the pressure head loss curve from a water meter typically installed at New Zealand homes (Kent PSMT 25mm). [28] Using this curve we calculate power dissipation in a water meter during a washing machine cycle, shower, and toilet flush; presented as Fig. 8. The total energy dissipated within the meter for each events is:

- 547 J per load of washing,
- 222 J per shower, and

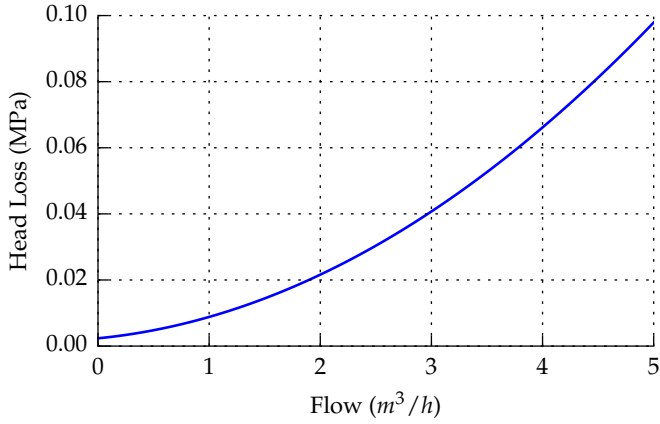


Fig. 7. Estimated head loss from a mechanical water meter typically installed in a domestic setting.

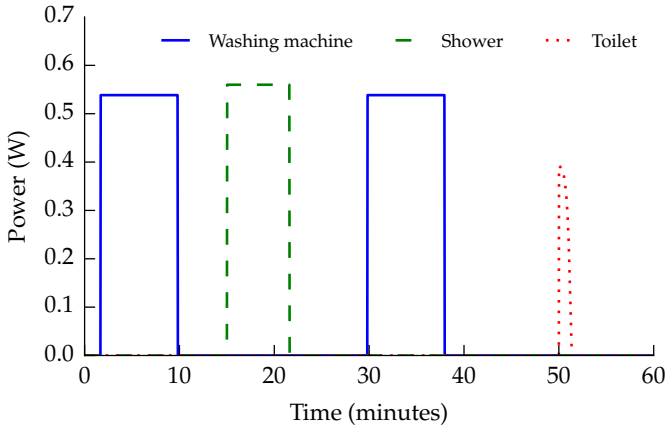


Fig. 8. Calculated power dissipation by a typical domestic mechanical water meter for each of the sample profile events.

- 24.3 J per flush of the toilet.

Over an average week the reference water meter would dissipate approximately 7.20 kJ of energy; averaging 1.03 kJ per day.

#### IV. ESTIMATION OF ENERGY REQUIREMENTS

In [29] we measure the energy efficiency of various low-power microcontrollers. Here we take measured data from that paper to estimate a smart meter's energy requirements. Measurements of an Atmel ATtiny 25V have been used as it offered good performance over a wide range of processor functions. A crude estimation of the processor's event loop is as follows:

- Sleep for 1 s (97.4 nJ)
- Execute 1000 instructions (1.14  $\mu$ J)
- Take 2 ADC measurements (2.56 nJ)
- Write 2 bytes to non-volatile memory (79.0  $\mu$ J)

Every six hours the device will transmit metered data by doing the following actions:

- Execute 1 000 000 instructions (1.14 mJ)
- Transmit 100 bytes of data over ZigBee radio (12.3 mJ)

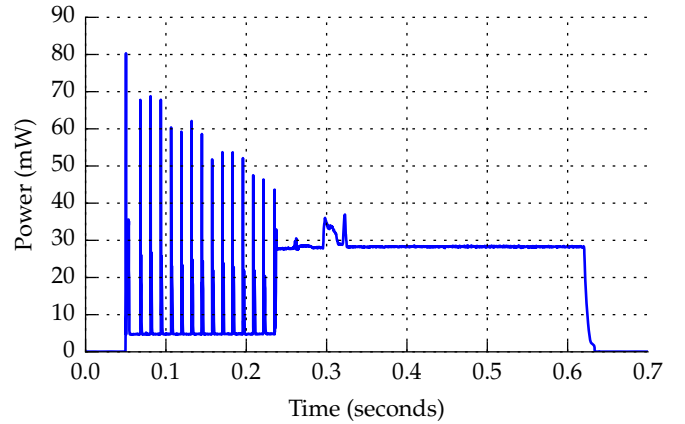


Fig. 9. Power draw from a ZigBee wireless module transmitting to a nearby receiver in optimal conditions. The ZigBee module is operated with a 3.3V supply voltage and is powered down between transmissions. The energy required to power-up the ZigBee module and transmit 100 bytes of data is 12.3 mJ.

- Write 10 bytes to non-volatile memory (394  $\mu$ J)

The energy requirements for a 100 byte data transmission over ZigBee (Digi International XBee S2) is presented as Fig. 9. This trace was recorded using a Tektronix TDC 2012 Digital Storage Oscilloscope across a 10.2  $\Omega$  current sense resistor.

Our estimation shows a monitoring and transmitting device would need about 6.96 J per day to operate in ideal transmission conditions. If the transmitter were to require one hundred times more energy to transmit, as an estimate of poor conditions, the energy requirements would jump to 9.39 J per day. It is therefore estimated that an energy harvester would need to deliver approximately 10 J of energy per day.

#### V. SIZING OF STREAMING CELL HARVESTER

We now estimate the physical size of a harvester capable of supplying enough energy to run an electronic water meter. We envision a harvester made from stacked layers of glass, each layer forming a rectangular channel similar to those constructed earlier. Such a harvester would be installed as shown in Fig. 10 to control the pressure loss within the harvester and to the consumer.

We know from Sections III and IV that an average of 1 kJ per day is dissipated inside a water meter and that we need to harvest 10 J for the electronic meter. This equates to an efficiency target of 1%.

Auckland tap water has a sodium content of 2.1–26.0  $\text{mg l}^{-1}$ . [30] This equates to a Debye length in the range 0.3–1.0 nm and therefore the optimum channel height between 0.6–2.1 nm.

We know from Section III that a typical shower consumes 7.50  $\text{l min}^{-1}$  for approximately 396 s. Using the head loss curve from Fig. 7, a flow rate of 7.50  $\text{l min}^{-1}$  would produce a pressure differential of 4.48 kPa. Therefore, a mechanical water meter dissipates a total of 222 J at a rate of 560 mW within the meter during a typical shower.



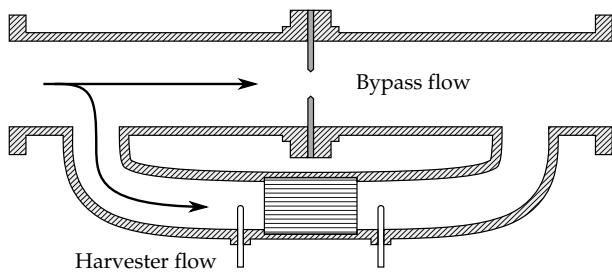


Fig. 10. Harvester schematic for the streaming cell harvester. Most water would bypass the harvester to prevent excessive pressure loss to the consumer. An orifice plate is inserted into the bypass to increase the pressure differential across the harvester.

This means a harvester must be capable of harvesting at least  $5.60 \text{ mW}$  at a pressure differential of  $4.48 \text{ kPa}$ . From the dimensions of the cell constructed and measured in Section II we can expect  $153 \text{ nW m}^{-1}$  of channel width at a pressure of  $260 \text{ kPa}$ . Fig. 4 confirms that the harvester output is linearly proportional to the pressure applied. We assume here that doubling the width of a channel will double the output power of the channel.

Normalising the cell's output for width and pressure yields  $588 \text{ pW m}^{-1} \text{ kPa}^{-1}$ . Therefore at our target pressure of  $4.48 \text{ kPa}$  we can expect output of  $2.64 \text{ nW m}^{-1}$ . Dividing the target output of  $5.60 \text{ mW}$  by this figure yields a required width of  $2.12 \times 10^6 \text{ m}$ . This equates to a harvester that, when packed into a cube, would have sides of  $3.17 \text{ m}$  in length.

## VI. CONCLUSION

The streaming cells fabricated in this paper achieved a conversion efficiency of approximately  $0.3 \mu\%$ . Stacking these cells into harvester capable of powering an electronic water meter would result in a cube having sides  $3.17 \text{ m}$  in length.

We have estimated that harvesting  $1\%$  of the power dissipated in a mechanical water meter would be sufficient to power an electronic water meter. In order to achieve this, such a cell would have to operate near the maximum predicted efficiency. Regardless of efficiency, it is expected that such narrow openings in domestic water feeds will eventually become clogged. We conclude that energy harvesting using readily fabricated streaming cells for the purpose of electronic meter reading is not yet practical.

Methods of inducing hydrodynamic slip at the interface may produce a more feasible streaming cell harvester design.

## REFERENCES

- [1] N. Chang, "Smart Gas And Water Meter Trends: Impacts on Meter Designs," *Metering International*, no. 4, pp. 38–39, 2012.
- [2] T. C. Britton, R. a. Stewart, and K. R. O'Halloran, "Smart metering: enabler for rapid and effective post meter leakage identification and water loss management," *Journal of Cleaner Production*, vol. 54, pp. 166–176, Sept. 2013.
- [3] B. Meters, "HydroLink Remote Reading Systems," 2014.
- [4] D. Stein, M. Kruihof, and C. Dekker, "Surface-Charge-Governed Ion Transport in Nanofluidic Channels," *Physical Review Letters*, vol. 93, pp. 1–4, July 2004.
- [5] G. B. Salieb-Beugelaar, K. D. Dorfman, A. van den Berg, and J. C. T. Eijkel, "Electrophoretic separation of DNA in gels and nanostructures," *Lab on a chip*, vol. 9, pp. 2508–23, Sept. 2009.
- [6] J. N. Israelachvili, *Intermolecular and Surface Forces*. Academic Press, 2011.
- [7] B. J. Kirby and E. F. Hasselbrink, "Zeta potential of microfluidic substrates: 1. Theory, experimental techniques, and effects on separations," *Electrophoresis*, vol. 25, pp. 187–202, Jan. 2004.
- [8] C.-C. Chang and R.-J. Yang, "Electrokinetic energy conversion in micrometer-length nanofluidic channels," *Microfluidics and Nanofluidics*, vol. 9, pp. 225–241, Dec. 2009.
- [9] H. Daiguji, Y. Oka, T. Adachi, and K. Shirono, "Theoretical study on the efficiency of nanofluidic batteries," *Electrochemistry Communications*, vol. 8, pp. 1796–1800, Nov. 2006.
- [10] H. Daiguji, P. Yang, A. J. Szeri, and A. Majumdar, "Electrochemomechanical Energy Conversion in Nanofluidic Channels," *Nano Letters*, vol. 4, pp. 2315–2321, Dec. 2004.
- [11] C. Davidson and X. Xuan, "Electrokinetic energy conversion in slip nanochannels," *Journal of Power Sources*, vol. 179, pp. 297–300, Apr. 2008.
- [12] C. Davidson and X. Xuan, "Effects of Stern layer conductance on electrokinetic energy conversion in nanofluidic channels," *Electrophoresis*, vol. 29, pp. 1125–30, Mar. 2008.
- [13] K. Hon, C. Zhao, C. Yang, and S. Low, "A method of producing electrokinetic power through forward osmosis," *Applied Physics Letters*, vol. 101, no. 14, p. 143902, 2012.
- [14] Y. Jiao, C. Yang, Y. Kang, and K. C. Hon, "Enhancement of Electrokinetic Power Generation by Surface Treatment on a Porous Glass," in *International Conference on Informatics, Environment, Energy and Applications*, vol. 66, (Shanghai, China), pp. 56–60, IPCBEE, 2014.
- [15] M.-C. Lu, S. Satyanarayana, R. Karnik, A. Majumdar, and C.-C. Wang, "A mechanical-electrokinetic battery using a nano-porous membrane," *Journal of Micromechanics and Microengineering*, vol. 16, pp. 667–675, Apr. 2006.
- [16] W. Olthuis, B. Schippers, J. Eijkel, and A. Vandenberg, "Energy from streaming current and potential," *Sensors and Actuators B: Chemical*, vol. 111–112, no. April, pp. 385–389, 2005.
- [17] J. Osterle, "Electrokinetic energy conversion," *Journal of Applied Mechanics*, pp. 161–164, 1964.
- [18] S. Pennathur, J. C. T. Eijkel, and A. van den Berg, "Energy conversion in microsystems: is there a role for micro/nanofluidics?," *Lab on a chip*, vol. 7, pp. 1234–7, Oct. 2007.
- [19] Y. Ren and D. Stein, "Slip-enhanced electrokinetic energy conversion in nanofluidic channels," *Nanotechnology*, vol. 19, p. 195707, May 2008.
- [20] F. H. J. van der Heyden, D. J. Bonthuis, D. Stein, C. Meyer, and C. Dekker, "Electrokinetic energy conversion efficiency in nanofluidic channels," *Nano Letters*, vol. 6, pp. 2232–7, Oct. 2006.
- [21] F. H. J. van der Heyden, D. J. Bonthuis, D. Stein, C. Meyer, and C. Dekker, "Power generation by pressure-driven transport of ions in nanofluidic channels," *Nano Letters*, vol. 7, no. 4, pp. 1022–1025, 2007.
- [22] Y. Xie, X. Wang, J. Xue, K. Jin, L. Chen, and Y. Wang, "Electric energy generation in single track-etched nanopores," *Applied Physics Letters*, vol. 93, no. 16, p. 163116, 2008.
- [23] J. Yang, F. Lu, L. Kostiuik, and D. Kwok, "Electrokinetic microchannel battery by means of electrokinetic and microfluidic phenomena," *Journal of Micromechanics . . .*, vol. 13, pp. 963–970, 2003.
- [24] J. Yang, F. Lu, L. W. Kostiuik, and D. Y. Kwok, "Electrokinetic Power Generation via Streaming Potentials in Microchannels: A Mobile-Ion-Drain Method to Increase Streaming Potentials," in *International Conference on MEMS, NANO and Smart Systems* (D. W. Badawy and D. W. Moussa, eds.), no. 780, (Banff, Alberta - Canada), pp. 675–679, IEEE, 2004.
- [25] G. Yongan and D. Li, "The  $\zeta$ -Potential of Glass Surface in Contact with Aqueous Solutions," *Journal of Colloid and Interface Science*, vol. 226, pp. 328–339, June 2000.
- [26] M. Heinrich and N. Isaacs, "Water Use in Auckland Households: Auckland Water Use Study (AWUS)," Tech. Rep. October 2008, BRANZ Ltd and WaterCare Services Ltd, 2008.
- [27] M. Heinrich, "Water End Use and Efficiency Project (WEEP): Final Report," Tech. Rep. 159, BRANZ Ltd, 2007.
- [28] Watercare New Zealand, "Private communication," 2014.
- [29] M. H. Jones and J. B. Scott, "The Energy Efficiency of 8-bit Low-power Microcontrollers," in *ENZCon 2011*, no. 1, (Palmerston North, New Zealand), pp. 87–90, ENZcon, 2011.
- [30] Watercare New Zealand, "Annual Water Quality Report 2012," tech. rep., 2012.